

Demonstration of a Discretely Tunable III-V-on-Silicon Sampled Grated DFB Laser

Sören Dhoore, *Student Member, IEEE*, Liyan Li, Amin Abbasi, *Student Member, IEEE*, Gunther Roelkens, *Member, IEEE*, and Geert Morthier, *Senior Member, IEEE*

Abstract—We demonstrate discrete wavelength tuning with a heterogeneously integrated III-V-on-silicon sampled grating distributed feedback laser. With only two injection currents, the laser is tunable over a wavelength range larger than 55 nm in wavelength steps of 5 nm. A maximum waveguide-coupled output power of 15 dBm is obtained as well as a high side mode suppression of more than 33 dB for all wavelength channels.

Index Terms—Distributed feedback lasers, tunable circuits and devices, hybrid integrated circuit bonding, silicon-on-insulator technology.

I. INTRODUCTION

WIDELY tunable laser diodes are expected to play a crucial role as light sources in future advanced optical networks. They can reduce the inventory cost as compared to fixed wavelength DFB lasers in WDM applications and offer additional functionality in optical access network architectures, where bandwidth can be dynamically assigned to users. Such next-generation optical access technology requires low-cost tunable laser diodes with sufficient tuning range and high optical output power [1].

In recent years there has been considerable research in the field of heterogeneously integrated III-V-on-silicon laser diodes, whereby laser structures are realised through incorporation of III-V gain material on the silicon-on-insulator (SOI) platform via direct or adhesive wafer bonding techniques [2]. The integration on SOI has the advantage that the lasers can be integrated with silicon passive waveguide circuits, high-speed silicon modulators and germanium photodetectors. As opposed to traditional InP-lasers, membrane III-V-on-silicon lasers allow the realization of gratings with a high coupling coefficient and strong optical confinement in the gain material.

Several III-V-on-silicon wavelength tunable lasers have been demonstrated already. These lasers typically make use of a set of heaters that allow to thermally tune the wavelength-selective filter characteristic of the laser structure.

Manuscript received June 2, 2016; revised July 14, 2016; accepted July 21, 2016. Date of publication July 22, 2016; date of current version September 28, 2016. This work was supported by the Methusalem Programme of the Flemish Government.

The authors are with the Photonics Research Group, Department of Information Technology, Interuniversity Microelectronics Center and the Center for Nano- and Biophotonics, Ghent University, Ghent 9000, Belgium (e-mail: soren.dhoore@intec.ugent.be; lili@intec.ugent.be; aamin@intec.ugent.be; gunther.roelkens@intec.ugent.be; geert.morthier@intec.ugent.be).

Color versions of one or more of the figures in this letter are available online at <http://ieeexplore.ieee.org>.

Digital Object Identifier 10.1109/LPT.2016.2593983

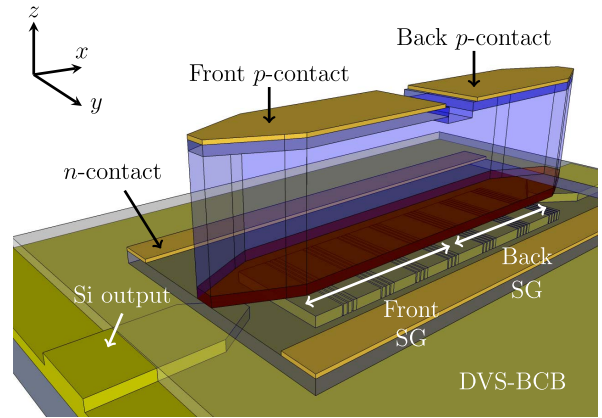


Fig. 1. 3D layout of the SG-DFB laser. The front and back SG have a slightly different periodicity to exploit the Vernier effect for wide wavelength tuning.

Examples include a laser structure with a double-ring resonator [3] and a structure containing a single-ring and a distributed Bragg reflector (DBR) mirror [4]. In another approach a combination of an arrayed waveguide grating (AWG) incorporated in the laser cavity and a set of semiconductor optical amplifiers (SOAs) is used to realise discrete wavelength tunability [5]. Yet another laser structure that makes use of 2 sampled grating DBR mirrors, a gain and a phase section to obtain over 13 nm wavelength tuning, has been presented in [6]. SG-DFB laser structures implemented on a pure III-V platform have been reported in [7] and [8].

In this letter we report on the experimental demonstration of a widely tunable sampled grating distributed feedback (SG-DFB) laser integrated on SOI. The presented laser is implemented as a two-section DFB laser and wavelength tuning is realised by variation of the currents injected into the two sections. This leads to rather simple wavelength control as compared to DBR lasers, which require an additional tuning current because of an extra phase section. The laser device is tunable over a wavelength range of more than 55 nm in discrete wavelength steps of 5 nm, with all wavelength channels having a side mode suppression ratio (SMSR) of more than 33 dB.

II. LASER DESIGN AND FABRICATION

The 3D layout of the SG-DFB laser structure is schematically shown in Fig. 1. The structure consists of a III-V

gain region that is integrated on top of an SOI waveguide circuit by means of adhesive DVS-BCB bonding [9]. The SOI waveguide structures are fabricated in a CMOS pilot-line at *imec* and have a 400 nm silicon device layer thickness with an etch depth of 180 nm. In this layer sampled gratings are implemented that provide optical feedback needed for lasing. The sampled gratings have a slightly different sampling period ($\Delta_{S,1}$ and $\Delta_{S,2}$) in order to exhibit a comb-like reflection spectrum with slightly different periodicity, which allows to exploit the Vernier effect for wide wavelength tuning. In our design $\Delta_{S,1}$ and $\Delta_{S,2}$ are chosen as 72 μm (10 sampling periods) and 80 μm (9 sampling periods) respectively. The total cavity length is 1440 μm . The second order gratings are 3.5 μm wide and have a period of 480 nm with a duty cycle of 75%, which corresponds to a Bragg wavelength of 1565 nm ($n_{\text{eff}} \approx 3.26$). Both sampled gratings have a sampling duty cycle d_{SG} of 10%, which ensures a sufficiently flat envelope of the reflection spectrum. This is needed to obtain a high side mode suppression across the entire tuning range [10].

The III-V epitaxial layer stack is a standard amplifier stack and consists of an n -InP bottom cladding layer (190 nm thick), six InGaAsP quantum wells (7 nm thick, 1.55 μm bandgap wavelength) surrounded by two InGaAsP separate confinement heterostructure layers (100 nm thick, 1.17 μm bandgap wavelength), a p -InP top cladding layer (1.5 μm thick) and a p^{++} -InGaAs top contact layer (200 nm thick).

In order to efficiently couple the light from the III-V region to the SOI output waveguides a double adiabatic tapered coupler, as described in [11], is used. The total III-V taper length is 200 μm and consists of two parts. In the first part the III-V waveguide is tapered down from 3 μm to 1 μm whereas the second part tapers from 1 μm to a taper tip of 600 nm. The underlying silicon rib waveguide tapers from 300 nm to 2 μm over a length of 150 μm .

The fabrication of the SG-DFB laser is similar to the fabrication of a standard III-V-on-silicon DFB laser and involves adhesive DVS-BCB bonding of the III-V epitaxy on the SOI waveguide structures. After the III-V substrate removal the laser structure is defined through a series of lithographic, wet/dry etching and metallisation steps. Detailed information on the fabrication process can be found in [12]. The p -contact consists of two individual contacts that allow independent current injection in the two sampled grating sections.

Upon carrier injection two counteracting effects come into play. The free-carrier plasma dispersion effect (very fast, $\sim \text{ns}$) induces a decrease in the refractive index due to an increase in the carrier density. As the carrier density is clamped above threshold only a limited change in carrier density can typically be achieved through current injection in the active layer. However, since the laser structure constitutes two sections, significant relative changes in the carrier density are possible through appropriate current variation in a push-pull manner. Self-heating (slow, $\sim \text{ms}$) on the other hand increases the refractive index. The presence of the buried oxide (BOX) layer in heterogeneously integrated III-V-on-silicon devices prevents efficient heat sinking and leads to devices with large thermal resistance. Based on thermal simulations with COMSOL the

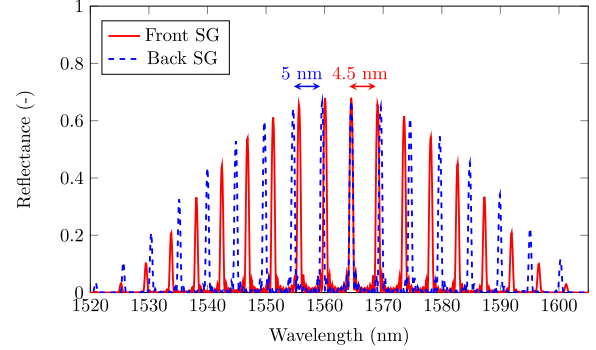


Fig. 2. Overlaid simulated reflection spectra for the two sampled gratings of the SG-DFB laser.

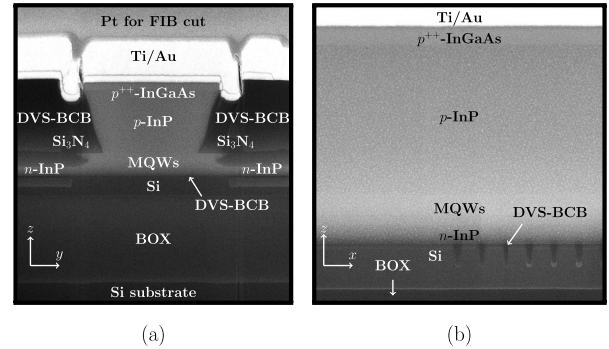


Fig. 3. SEM image of the fabricated SG-DFB laser. (a) Transverse cross-sectional view; (b) Longitudinal cross-sectional view.

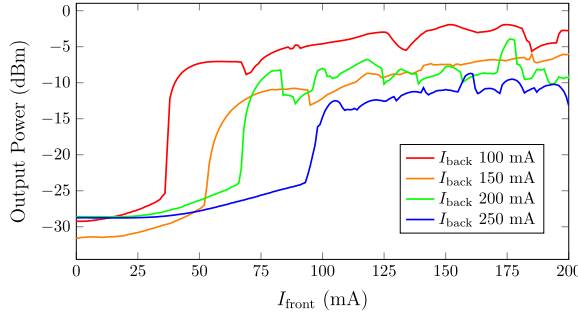
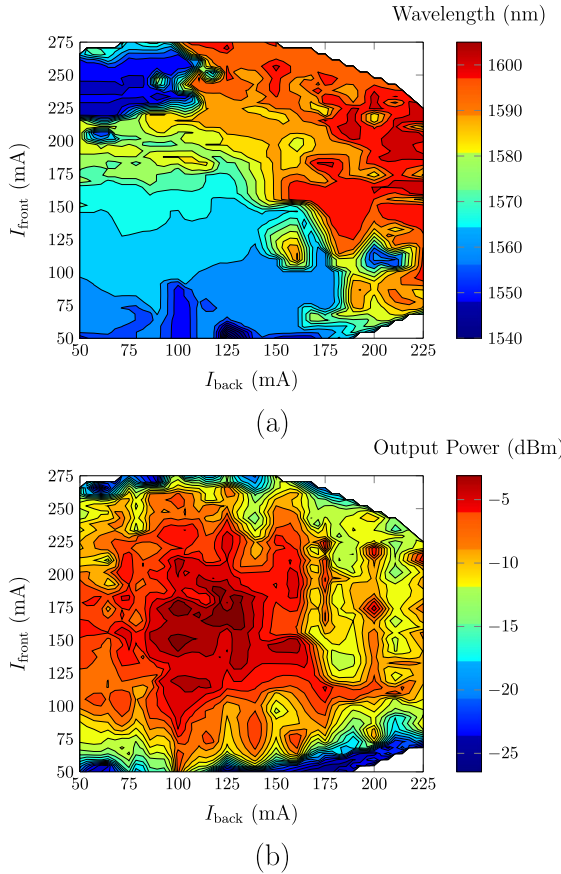
thermal resistance of the SG-DFB laser can be estimated to be 0.124 K/mW.

Figure 2 shows the overlaid simulated reflection spectra for both sampled gratings of the SG-DFB laser. The simulations are based on the transfer-matrix method [13] and optical mode calculations with FIMMWAVE, a mode solver from PhotonDesign [14]. The front grating reflector has a designed free spectral range ($\text{FSR}_{\text{front}}$) of 5 nm. For the back grating reflector the designed free spectral range (FSR_{back}) is 4.5 nm. The small difference in FSR of 0.5 nm creates a Vernier effect and allows wide wavelength tuning. The limitation on the tuning range is set by the repeat mode spacing ($\text{FSR}_{\text{repeat}}$) and can be estimated from [15]

$$\text{FSR}_{\text{repeat}} = \frac{\text{FSR}_{\text{front}} \cdot \text{FSR}_{\text{back}}}{\text{FSR}_{\text{front}} - \text{FSR}_{\text{back}}} = 45 \text{ nm}. \quad (1)$$

In order to achieve quasi-continuous tuning with full wavelength coverage, the change in effective index upon carrier injection should be large enough to directly tune over at least the mode spacing of a single reflector, i.e. over $\text{FSR}_{\text{back}} = 4.5 \text{ nm}$.

Figures 3(a) and 3(b) respectively show a transverse and longitudinal cross-sectional SEM image of the fabricated SG-DFB laser device, captured in the center of the laser cavity. The laser mesa has a V-shape, which is realised through wet etching of the p -InP cladding layer. This increases the optical confinement factor in the MQWs (12% confinement factor in the 6 quantum wells) and realizes narrow taper tips. The total

Fig. 4. Light-current (*LI*) characteristics of the SG-DFB laser.Fig. 5. Tuning characteristics of the SG-DFB laser. (a) Lasing wavelength versus I_{front} and I_{back} ; (b) Fiber-coupled output power versus I_{front} and I_{back} .

DVS-BCB bonding layer thickness is 40 nm, which gives rise to a relatively large effective grating coupling constant $\kappa_{\text{eff}} = \kappa \cdot d_{\text{SG}}$ that (based on simulations with the measured laser structure dimensions) is estimated to be 31.8 cm^{-1} .

III. DEVICE AND TUNING CHARACTERISTICS

Characterisation of the laser device is done at a heatsink temperature of 10°C . Through a standard fiber-to-chip SOI grating coupler light is coupled from the laser to a standard single-mode optical fiber. The measured fiber-to-chip coupling efficiency is -9 dB at 1550 nm and decreases monotonically, with a coupling efficiency of -18 dB at 1600 nm . Using a current source and three electrical DC probes the front

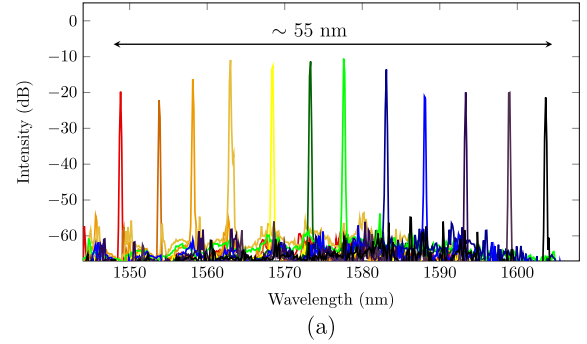


Fig. 6. (a) Superimposed lasing spectra; (b) Fiber-coupled output power and SMSR at the different wavelength channels.

(I_{front}) and back (I_{back}) sampled-grating section of the laser are independently biased.

The series resistance of both laser sections (dV/dI_{front} and dV/dI_{back}) is 6Ω . The resistance between the two *p*-contacts is 250Ω . The light-current (*LI*) characteristics of the SG-DFB laser are shown in Fig. 4. Thereby I_{front} is swept while I_{back} is kept constant. At $(I_{\text{front}}, I_{\text{back}}) = (175 \text{ mA}, 100 \text{ mA})$ the fiber-coupled output power is -1.94 dBm . The threshold current increases with increasing I_{back} because of heating and deteriorated overlap of the reflection peaks of both reflectors upon current injection. For uniform pumping ($I_{\text{front}} = I_{\text{back}}$) the total threshold current is 90 mA . The ripples in the *LI*-curves are attributed to mode hopping.

Figures 5(a) and 5(b) show the lasing wavelength and fiber-coupled output power versus I_{front} and I_{back} . Generally the lasing wavelength increases with total injection current $I_{\text{tot}} = I_{\text{front}} + I_{\text{back}}$ due to the dominant heating effect, as discussed in section II. At a total injection current $I_{\text{tot}} = 275 \text{ mA}$ the fiber-coupled output power reaches maximum values between -3 dBm and -1.8 dBm . Hence the maximum output power in the silicon waveguide can be estimated to be about 15 dBm . This yields a (single-sided) wall-plug efficiency of 4% . At larger injection currents the power drops again due to local heating.

Figure 6(a) shows the superimposed lasing spectra across the wavelength tuning range. Lasing occurs from 1547 to 1603 nm , at a discrete number of wavelengths. The spacing between these wavelength channels is 5 nm and corresponds with the designed peak spacing, as discussed in section II. Table I shows the injection current and lasing wavelength for the different channels shown in Fig. 6. Around each

TABLE I
INJECTION CURRENT AND LASING WAVELENGTH FOR
THE CHANNELS SHOWN IN FIG. 6

Channel	I_{front} (mA)	I_{back} (mA)	I_{tot} (mA)	λ (nm)
1	50	235	285	1548.83
2	90	265	355	1553.79
3	140	80	220	1558.14
4	100	135	235	1563.01
5	115	170	285	1568.47
6	125	185	310	1573.34
7	100	210	310	1577.60
8	150	220	370	1583.11
9	160	245	405	1588.02
10	180	115	295	1593.34
11	160	165	325	1599.03
12	225	160	385	1603.66

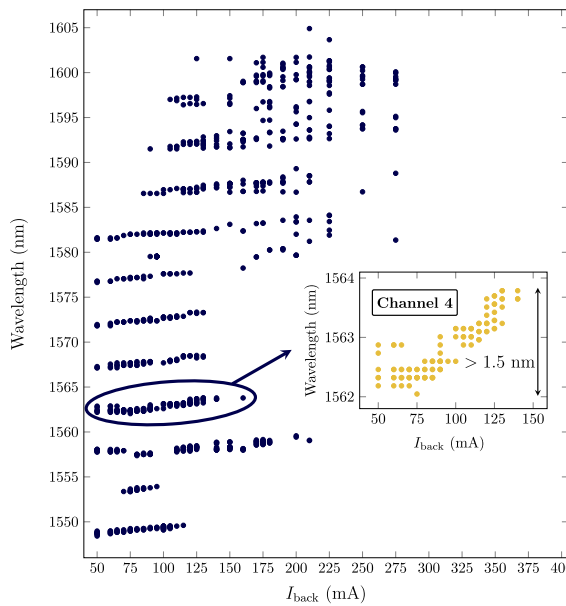


Fig. 7. Illustration of quasi-continuous wavelength tuning at the different wavelength channels. I_{front} is implicit. The inset shows an enlarged plot for Channel 4.

wavelength channel about 1.5 nm quasi-continuous tuning is possible. This is clarified in Fig. 7, which shows the lasing wavelength versus I_{back} , with I_{front} implicit. The inset shows an enlarged plot for Channel 4. All channels operate in single mode regime with a SMSR ranging from 33 dB to 48 dB. The fiber-coupled output power varies from -12 dBm to -2.8 dBm. This is illustrated in Fig. 6(b), which shows the fiber-coupled output power and SMSR for the different wavelength channels. The variation in the fiber-coupled output power is due to the variation of the total current for all wavelength channels and due to the influence of the grating coupler response. Also note that the overall wavelength tuning range of 55 nm is larger than the predicted 45 nm. This may be attributed to the limited bandwidth of the gain spectrum

(that red shifts at high injection currents). In this way lasing is most likely to occur near the gain peak with good suppression of the repeat modes at shorter wavelengths.

IV. CONCLUSION

A novel III-V-on-silicon SG-DFB laser has been experimentally demonstrated. The laser is tunable over a wide wavelength range of 55 nm in discrete steps of 5 nm. Due to the limited achievable change in carrier density upon current injection and the large thermal impedance of the device no wide, continuous tuning could be obtained. However, with a redesign of the sampled gratings and improvements in the thermal heat sinking this problem can be addressed. The presented laser device may find application as tunable laser source in future optical access networks.

ACKNOWLEDGMENTS

The authors thank L. Van Landschoot for the FIB images and S. Verstuyft and M. Muneeb for help with metallisation for contacting of the devices.

REFERENCES

- [1] K. Grobe, M. H. Eiselt, S. Pachnicke, and J.-P. Elbers, "Access networks based on tunable lasers," *J. Lightw. Technol.*, vol. 32, no. 16, pp. 2815–2823, Aug. 15, 2014.
- [2] G. Roelkens *et al.*, "III-V/silicon photonics for on-chip and intra-chip optical interconnects," *Laser Photon. Rev.*, vol. 4, no. 6, pp. 751–779, 2010.
- [3] J. C. Hulme, J. K. Doylend, and J. E. Bowers, "Widely tunable Vernier ring laser on hybrid silicon," *Opt. Exp.*, vol. 21, no. 17, pp. 19718–19722, 2013.
- [4] S. Keyvaninia *et al.*, "Demonstration of a heterogeneously integrated III-V/SOI single wavelength tunable laser," *Opt. Exp.*, vol. 21, no. 3, pp. 3784–3792, 2013.
- [5] A. L. Liepvre *et al.*, "Wavelength selectable hybrid III-V/Si laser fabricated by wafer bonding," *IEEE Photon. Technol. Lett.*, vol. 25, no. 16, pp. 1582–1585, Aug. 15, 2013.
- [6] M. N. Sysak, J. O. Anthes, J. E. Bowers, O. Raday, and R. Jones, "Integration of hybrid silicon lasers and electroabsorption modulators," *Opt. Exp.*, vol. 16, no. 17, pp. 12478–12486, 2008.
- [7] S. Kim, Y. Chung, S.-H. Oh, and M.-H. Park, "Design and analysis of widely tunable sampled grating DFB laser diode integrated with sampled grating distributed Bragg reflector," *IEEE Photon. Technol. Lett.*, vol. 16, no. 1, pp. 15–17, Jan. 2004.
- [8] N. Nunoya *et al.*, "Tunable distributed amplification (TDA-) DFB laser with asymmetric structure," *IEEE J. Sel. Topics Quantum Electron.*, vol. 17, no. 6, pp. 1505–1512, Nov./Dec. 2011.
- [9] S. Keyvaninia, M. Muneeb, S. Stanković, P. Van Veldhoven, D. Van Thourhout, and G. Roelkens, "Ultra-thin DVS-BCB adhesive bonding of III-V wafers, dies and multiple dies to a patterned silicon-on-insulator substrate," *Opt. Mater. Exp.*, vol. 3, no. 1, pp. 35–46, 2013.
- [10] J. Buus, M.-C. Amann, and D. J. Blumenthal, *Tunable Laser Diodes and Related Optical Sources*. New York, NY, USA: Wiley, 2005.
- [11] M. Lamponi *et al.*, "Low-threshold heterogeneously integrated InP/SOI lasers with a double adiabatic taper coupler," *IEEE Photon. Technol. Lett.*, vol. 24, no. 1, pp. 76–78, Jan. 1, 2012.
- [12] S. Keyvaninia *et al.*, "Heterogeneously integrated III-V/silicon distributed feedback lasers," *Opt. Lett.*, vol. 38, no. 24, pp. 5434–5437, 2013.
- [13] L. A. Coldren, S. W. Corzine, and M. L. Mashanovitch, *Diode Lasers and Photonic Integrated Circuits*. New York, NY, USA: Wiley, 2012.
- [14] *Photon Design*. (2011). [Online]. Available: <http://www.photond.com>
- [15] S. Matsuo and T. Segawa, "Microring-resonator-based widely tunable lasers," *IEEE J. Sel. Topics Quantum Electron.*, vol. 15, no. 3, pp. 545–554, May/Jun. 2009.